Quantum Global Positioning Systems

The Quantum Widget Company ©

Contact: qwidgetco.com/about

December 13, 2017

Abstract

In this white paper we discuss the role of quantum algorithms in Global Positioning Systems (GPS), particularly for the purposes of the optimal routing and scheduling of autonomous technologies. The optimal trajectories for these autonomous technologies as they visit different targets to perform particular tasks is determined via quantum annealing on a DWave 2000Q quantum computer. Moreover, our software results are shown to have applications with novel quantum hardware technologies, such as the Polariton Interferometer, which paves the route towards quantum GPS. Networks of these quantum sensor technologies are shown to introduce a new GPS paradigm, providing autonomous control in a variety of commercial settings.

Introduction

The Quantum Widget Company is comprised of physicists, mathematicians, engineers, and software developers from all over the world. We are passionate and committed to solving unique problems with novel quantum software solutions. Quantum science and machine learning technology has gained increasing popularity over the past few decades. With the arrival of Noisy Intermediate-Scale-Quantum Computers (NISQs) in the commercial marketplace, the integration of classical machine learning with quantum computing is financially attractive. The DWave NISQ is a 2000-qubit quantum annealer (QA), which solves optimization problems (e.g., optimal routing and scheduling of unmanned aerial vehicles, delivery trucks or flight control). Opportunities to gain advantage in a quantum paradigm of parcel delivery can be realized via our unique approach to autonomous vehicle optimization. Recently, we have developed a quantum branch and bound optimization algorithm for assigning cooperating homogeneous uninhabited aerial vehicles to multiple tasks [1], which has been implemented on a DWave NISQ. Our product provides customers with a way to determine the optimal paths (trajectories) that autonomous technologies should follow when they perform tasks on given targets (e.g., drones). This product, combined with our novel quantum sensing technologies [2], facilitates the development of Quantum Global Positioning Systems (GPS) [3], and solutions to the path optimization (traveling salesman) problem [4], among others. Currently, we are using the DWave NISQ for delivering quantum machine learning solutions to the customer.

Roadmap

I. Commercial Applications

Assigning tasks to a set of autonomous technologies is a critical component of many commercial endeavors (e.g., Amazon Prime Air, Greyhound, UPS, etc.) and is usually performed by humans. However, if the commercial endeavor must be carried out in a place with harsh conditions for humans, and/or with limited communication access, the decision making procedure is typically done by a computer with outdated classical algorithms, or the task is simply not feasible to perform. Also, if the amount of information is too large, e.g. there are hundreds of vehicles operating at the same time, it may not viable for a human to consider all the scenarios and make the right decision within a reasonable amount of time. Consequently, the need for autonomous decision making becomes prevalent. The autonomous decision making problem can be stated as a propositional problem, which is NP-hard and can be mapped onto an Ising Hamiltonian [5]. As such, we present a 2D version of the autonomous optimization problem, which delivers a visualization of how QA can be used to obtain an ideal schedule for the autonomous technologies.

A. D-Wave

For the present work, we use a DWave 2000Q to execute and solve our novel quantum branch and bound optimization algorithm. The DWave 2000Q architecture is explained in Ref. [6]. Concrete problems are mapped in to the Ising spin model (a minimization problem), by considering logical gates as Boolean clauses and transforming these clauses into arithmetic expressions, where binary values $(0, 1)$ map to spin values $(-1, 1)$, respectively. The end result is an energy function $E(s)$, defined on $(-1, 1)$, that has a minimum energy when the corresponding binary values $(0, 1)$ satisfy all the clauses [7].

B. Unmanned Autonomous Vehicles

Generally speaking, Unmanned Autonomous Vehicles (UAVs) are moving with a velocity $v_i(t)$, and an angle $\theta_i(t)$, such that they must go from one place to another, and be in those places with a specific inclination. For example, if the UAV has a sensor, then when the vehicle arrives at the desired location the sensor must face the sample. To further simplify the problem, let us suppose that the vehicle moves with constant speed v and has a maximum rate of turn (angular velocity) ω^{max}. As such, the dynamics of the $i-$th vehicle can be described by the set of differential equations:

$$\dot{x}_i = v_i \cos(\theta_i), \tag{1}$$
$$\dot{y}_i = v_i \sin(\theta_i), \tag{2}$$
$$\dot{\theta}_i = \omega^{max} u;\ u \in \{-1, 0, 1\}, \tag{3}$$
$$\dot{v}_i = 0. \tag{4}$$

The angular velocity is taken at the maximum because this guarantees finding the maximum curvature path, which is equivalent to finding the minimum length path under these assumptions. The UAV has a finite amount of fuel, which means that there is another constraint on the amount of time traveled by a given UAV. As a simple example, we benchmark a single vehicle that has to visit 4 colinear targets, each of which must be visited at a specific inclination. Also, the maximum radius of turn is given by 0.5 in arbitrary units. There are a total of $4! = 24$ ways in which the vehicle can visit the 4 targets as shown in Figure 1. There are three paths that lead to the same amount of consumed fuel, and they are marked with the minimum distance, which is 9.644. The proposed method in Ref. [8] defines a binary variable that allows a transformation of this optimization problem to a Quadratic Unconstrained Binary Optimization (QUBO) problem:

$$z_{i,\alpha} = \begin{cases} 1 & \text{if target } i \text{ is the } \alpha\text{-th site visited on the tour,} \\ 0 & \text{otherwise.} \end{cases} \tag{5}$$

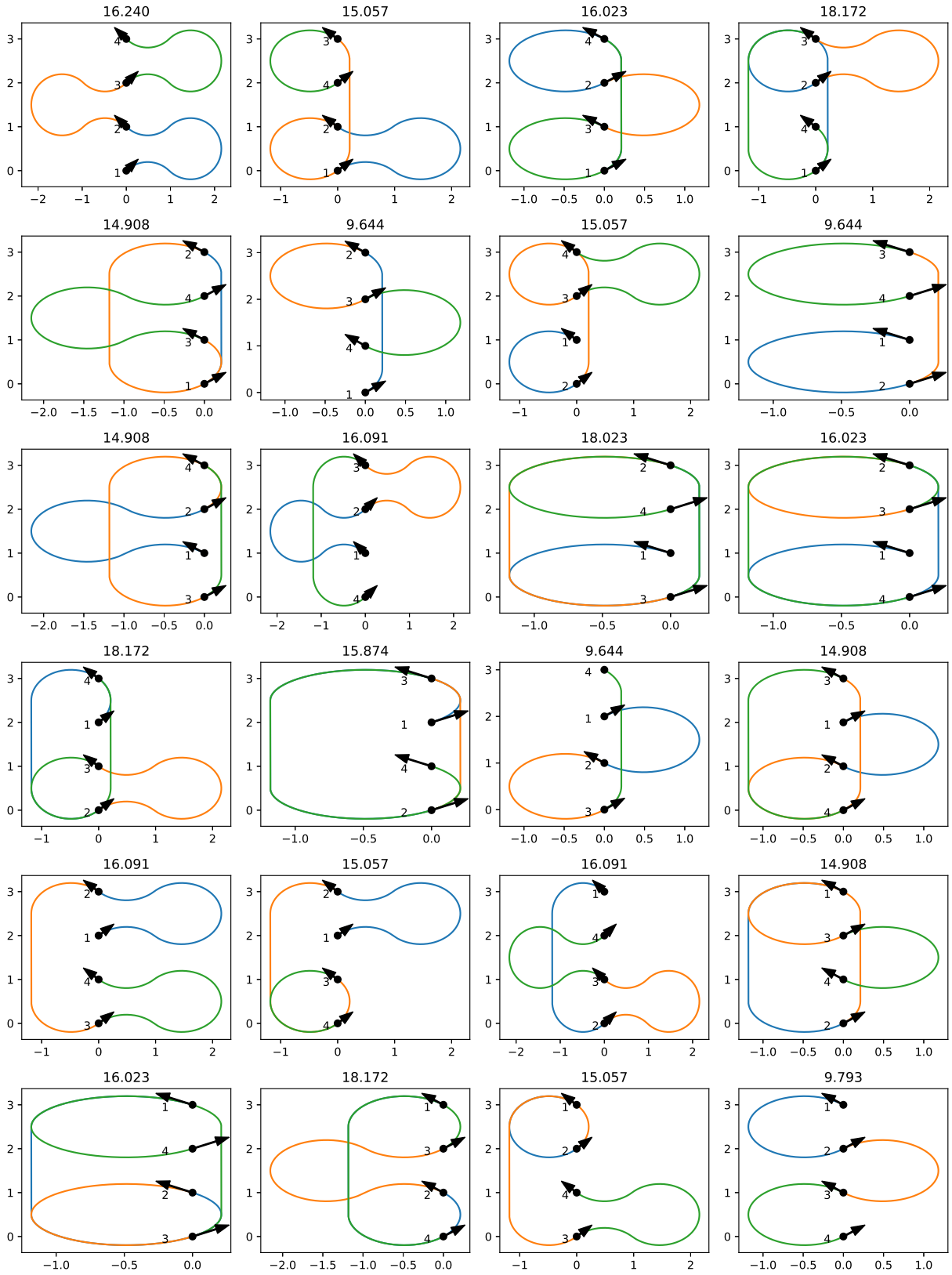

Figure 1: *Possible paths of a UAV starting at location 1, then going to 2, etc. The total distance, in arbitrary units is shown above each graphic. The specific inclination is shown with an arrow at each point.*

With this binary variable it is possible to define the quantum branch and bound optimization problem as

$$E = \sum_{ij\alpha} d_{i,j} z_{i,\alpha} (z_{j,\alpha+1} + z_{j,\alpha-1}), \tag{6}$$

where $d_{i,j}$ is the distance between the i-th and the j-th target, subject to the constrains

$$\sum_i z_{i,\alpha} = \sum_\alpha z_{i,\alpha} = 1. \tag{7}$$

This implies that only one target is visited in each position of the tour and that the $i-$th target is visited exactly once during the tour, i.e., there is a one-to-one correspondence of target-position pairs in the tour. The constrains are therefore equivalent to

$$\sum_i z_{i,\alpha} - 1 = 0, \qquad \sum_\alpha z_{i,\alpha} - 1 = 0, \tag{8}$$

$$\implies W_1 \left(\sum_i z_{i,\alpha} - 1 \right)^2 = 0, \qquad W_2 \left(\sum_\alpha z_{i,\alpha} - 1 \right)^2 = 0. \tag{9}$$

These terms can be added to the energy to be optimized. Here W_1 and W_2 are weights that should be set to $N\langle d_{i,j} \rangle$ so that they are of the same order as the term (6). Thus, the new optimization problem is

$$E = \sum_{ij\alpha} d_{i,j} z_{i,\alpha} (z_{j,\alpha+1} + z_{j,\alpha-1}) + N\langle d_{i,j} \rangle \sum_\alpha \left(\sum_i z_{i,\alpha} - 1 \right)^2 + N\langle d_{i,j} \rangle \sum_i \left(\sum_\alpha z_{i,\alpha} - 1 \right)^2. \tag{10}$$

In our example, we have a non-symmetric distance matrix that is shown in Figure 2.

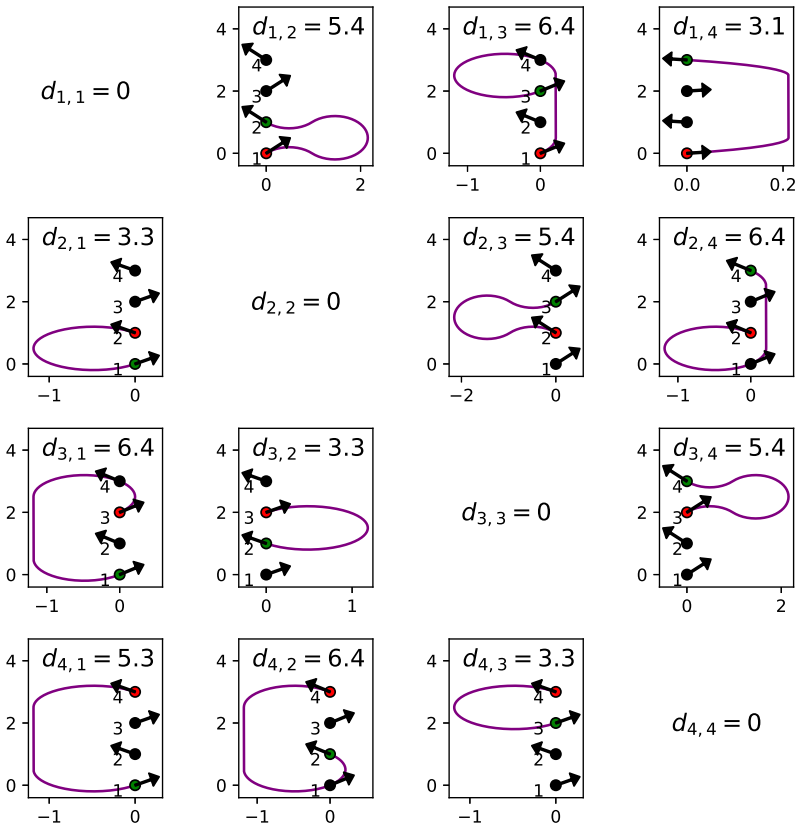

Figure 2: *Distances in arbitrary units from the starting red point to the finishing green point.*

From the optimization problem Eq. (10), we obtain the biases and couplings between the QUBO variables. For instance, the diagonal terms of the z matrix are accompanied by the QUBO variables biases. The first term only contains crossed terms, while the second and third terms of Eq. (10) contain the monomials

$$N\langle d_{i,j}\rangle \sum_{\alpha,i}(-z_{i,\alpha}) + N\langle d_{i,j}\rangle \sum_{i,\alpha}(-z_{i,\alpha}) = -2N\langle d_{i,j}\rangle \sum_{i,\alpha} z_{i,\alpha}, \tag{11}$$

which implies that the biases of the QUBO variables are $-2N\langle d_{i,j}\rangle$. It can be seen from examining the couplings that they are present in the three terms on the RHS of Eq. (10). In the second term of the RHS of Eq. (10) we have crossed terms:

$$N\langle d_{i,j}\rangle \sum_{\alpha}\sum_{i=1}^{N}\sum_{j=i+1}^{N} 2z_{i,\alpha}z_{j,\alpha}, \tag{12}$$

and in the third term we have crossed terms:

$$N\langle d_{i,j}\rangle \sum_{i}\sum_{\alpha=1}^{N}\sum_{\beta=\alpha+1}^{N} 2z_{i\alpha}z_{i,\beta}. \tag{13}$$

Here, it should be pointed out that any two QUBO variables with the same target index and different position index or with the same position index but different target index have a base coupling value of $2N\langle d_{i,j}\rangle$. Moreover, there are corrections to some of those couplings, as well as new couplings given by the first term on the RHS of Eq. (10), which is the most intricate coupling. Here, the crossed terms always have a different position index, so there are two distinct cases: if they have equal target index, the crossed terms correspond to corrections of the latter couplings, otherwise, the crossed terms correspond to new couplings. It should also be noted that the corrections to the latter couplings are zero, because if the crossed terms have equal target index, then the added weight will be $d_{i,i} = 0$. Consequently, the new remaining couplings are given by:

$$\begin{aligned}
&\sum_{\substack{ij\\ i\neq j}}\sum_{\alpha=1}^{N-1} d_{i,j}z_{i,\alpha}z_{j,\alpha+1} + \sum_{\substack{ij\\ i\neq j}}\sum_{\alpha=2}^{N} d_{i,j}z_{i,\alpha}z_{j,\alpha-1} = \sum_{\substack{ij\\ i\neq j}}\sum_{\alpha=1}^{N-1} d_{i,j}z_{i,\alpha}z_{j,\alpha+1} + \sum_{\substack{ij\\ i\neq j}}\sum_{\alpha=1}^{N-1} d_{i,j}z_{i,\alpha+1}z_{j,\alpha}\\
&\quad = 2\sum_{\substack{ij\\ i\neq j}}\sum_{\alpha=1}^{N-1} d_{i,j}z_{i,\alpha}z_{j,\alpha+1} = 2\sum_{\alpha=1}^{N-1}\left(\sum_{i=1}^{N}\sum_{j=i+1}^{N} d_{i,j}z_{i,\alpha}z_{j,\alpha+1} + \sum_{j=1}^{N}\sum_{i=j+1}^{N} d_{i,j}z_{i,\alpha}z_{j,\alpha+1}\right)\\
&\quad = 2\sum_{\alpha=1}^{N-1}\left(\sum_{i=1}^{N}\sum_{j=i+1}^{N} d_{i,j}z_{i,\alpha}z_{j,\alpha+1} + \sum_{i=1}^{N}\sum_{j=i+1}^{N} d_{j,i}z_{j,\alpha}z_{i,\alpha+1}\right).
\end{aligned} \tag{14}$$

From Eq. (14) it is possible to obtain the new remaining couplings. Our treatment of the optimization problem also allows for us to provide the customer with an explanation of a general problem for the case where there are N targets.

C. Mapping the problem onto Chimera graph

We next write a Quantum Macro Assembler (QMASM) file to map the problem into the Chimera Graph [9]. The QMASM has as its inputs the biases and couplings between the QUBO variables, i.e. qubits; then it maps this problem onto the DWave 2000Q Chimera Graph. Finally, QMASM runs the problem on the DWave 2000Q computer.

This yields the following solution:

```
Solution #1 (energy = -89.81, tally = 5):

    Name  Spin  Boolean
    ----  ----  --------
    Z11     -1  False
    Z12     -1  False
    Z13     +1  True
    Z14     -1  False
    Z21     -1  False
    Z22     +1  True
    Z23     -1  False
    Z24     -1  False
    Z31     +1  True
    Z32     -1  False
    Z33     -1  False
    Z34     -1  False
    Z41     -1  False
    Z42     -1  False
    Z43     -1  False
    Z44     +1  True
```

which shows the name of each qubit and whether they have a 0 value (False) or a 1 value (True).

Target	Position in the tour
1	3
2	2
3	1
4	4

From the definition of the binary variables as seen in Eq. (5), this solution corresponds to the path shown in row 4, column 3 of Figure 1, which indeed has the minimum distance.

II. The Polariton Interferometer

The Polariton Interferometer is a novel quantum Inertial Measurement Unit (IMU) [10], that provides the following bias instabilities (BI):

$$\mathrm{BI}_{\dot{x}_i} \sim 10^{-3}\ [\mathrm{m}\cdot\mathrm{hr}^{-1}], \tag{15}$$

$$\mathrm{BI}_{\dot{y}_i} \sim 10^{-3}\ [\mathrm{m}\cdot\mathrm{hr}^{-1}], \tag{16}$$

$$\mathrm{BI}_{\dot{\theta}_i} \sim 10^{-3}\ [^{\circ}\cdot\mathrm{hr}^{-1}]. \tag{17}$$

Moreover, the Polariton Interferometer acheives an Angle Random Walk (ARW) of

$$\mathrm{ARW} \sim 10^{-5}\ [^{\circ}\cdot\mathrm{s}^{-1}\cdot\mathrm{Hz}^{-1/2}], \tag{18}$$

and a Velocity Random Walk (VRW) of

$$\mathrm{VRW} \sim 10^{-5}\ [\mathrm{m}\cdot\mathrm{s}^{-1}\cdot\mathrm{Hz}^{-1/2}]. \tag{19}$$

Eqs. (18)- (19) can be used in Eqs. (1)- (3) to acheive a quantum Global Positioning System (qGPS). This qGPS relies on the interference of exciton-polariton quasi-particles to determine the trajectories of UAVs with quantum precision. It exhibits significant advantages over traditional GPS and IMU systems, for it operates independently

from GPS satellites which need to correct for measurement errors. In summary, the Polariton Interferometer works by pulsing light through a micrometer-sized component which alters the light that passes through it. This light is then passed through a thin film microcavity where a polariton condensate is formed. Afterwards, an interference pattern is induced that allows the rotational and acceleration rate of the device to be detected. Accordingly, the Polariton Interferometer is an on-chip, quantum accurate IMU. These quantum accurate measurements can then be integrated with the DWave 2000Q machine learning optimization algorithms for UAV swarm optimization.

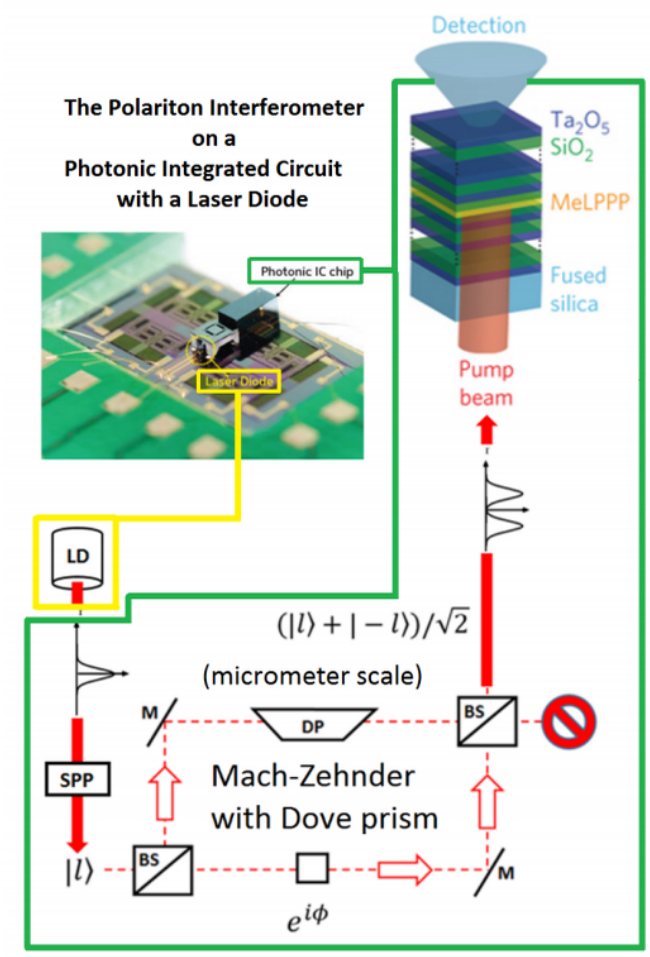

Figure 3: *Schematic diagram of the Polariton Interferometer*

One of the commercially attractive features of the Polariton Interferometer is that it can achieve unparalleled accuracy at room temperatures, unlike competing quantum technologies.

Conclusions

We have developed algorithms that provide our customer with a trajectory optimization description for Autonomous Unmanned Vehicles (UAVs) performing several tasks on several targets. In addition to the algorithm itself, and our ability to solve it using quantum annealing (implemented on DWave 2000Q), we have also developed a quantum Global Positioning System (qGPS) paradigm that provides the customer with the necessary accuracy when it comes to determining the position and direction the aforementioned UAVs. We have outlined how networks of quantum sensors, namely Polariton Interferometers, can be used to improve results over the state of the art GPS.

References

[1] Rasmussen, S.J. and Shima, T., Branch and bound tree search for assigning cooperating UAVs to multiple tasks. In IEEE American Control Conference, pp. 6 (2006).

[2] Moxley III, F.I., Frederick Ira Moxley III, Room-temperature exciton-polariton superfluid quantum interference device and quatron-polariton superconducting quantum interference device. U.S. Patent Application 15/402,149 (2017).

[3] Marks, P., Quantum positioning system steps in when GPS fails (2014).

[4] Warren, R.H., Small Traveling Salesman Problems. Journal of Advances in Applied Mathematics, 2(2) (2017).

[5] Kaminsky, W.M. and Lloyd, S., Scalable architecture for adiabatic quantum computing of NP-hard problems. Quantum computing and quantum bits in mesoscopic systems, pp.229-236 (2004).

[6] Sid, N. and Release, S. *Getting Started With the D-Wave*, 1(604), pp. 112 (2008).

[7] Warren, R.H., Gates for Adiabatic Quantum Computing. arXiv preprint arXiv:1405.2354 (2014).

[8] Smelyanskiy, V.N., Rieffel, E.G., Knysh, S.I., Williams, C.P., Johnson, M.W., Thom, M.C., Macready, W.G. and Pudenz, K.L., A near-term quantum computing approach for hard computational problems in space exploration. arXiv preprint arXiv:1204.2821 (2012).

[9] Scott Pakin. A Quantum Macro Assembler. In Proceedings of the 20th Annual IEEE High Performance Extreme Computing Conference (HPEC 2016), DOI: 10.1109/HPEC.2016.7761637.

[10] Moxley III, F.I., Dowling, J.P., Dai, W. and Byrnes, T., Sagnac interferometry with coherent vortex superposition states in exciton-polariton condensates. Physical Review A, 93(5), p.053603 (2016).